On the structure and dynamics of secondary *n*-alkyl cations

Allan L. L. East,[1,a)] Tomáš Bučko,[2] and Jürgen Hafner[2]

[1]*Department of Chemistry and Biochemistry, University of Regina, Regina, Saskatchewan S4S 0A2, Canada*
[2]*Faculty of Physics and Centre for Computational Materials Science Materialphysik, Universität Wien, Sensengasse 8, A-1090 Wien, Austria*

A variety of computational studies was undertaken to examine and establish the relative importance of open versus closed structures for unbranched secondary *n*-alkyl cations. First, the PW91 level of density functional theory was used to optimize over 20 minimum-energy structures of *sec*-pentyl, *sec*-hexyl, and *sec*-heptyl ions, demonstrating that closed structures are more stable than open ones on the potential energy surface (PES). Second, PW91 was used with a theoretical Andersen thermostat to perform a molecular dynamics simulation (150 ps) of $C_9H_{19}^+$ at a typical catalytic temperature of 800 K, demonstrating that the structure preference is *inverted* on the free-energy surface. Third, both quantum (rigid-rotor/harmonic oscillator) and classical partition functions were used to demonstrate that the simulated structure-opening at catalytic temperatures is due to the floppiness of the open forms, which improves its free energy by both lowering its zero-point vibrational energy and increasing its molecular entropy. The particular conformer of the preferred open form (at 800 K) is dependent on length of alkyl ion, with pentyl ions preferring syn/anti structures but longer ions preferring open-clinal ones. These results, plus an additional set of PES optimized structures from an alternative level of theory (MP2/6-31G(d,p)), are used to discuss the likely nature of secondary *n*-alkyl ions. © *2009 American Institute of Physics.*
[doi:10.1063/1.3230603]

I. INTRODUCTION

Computational chemistry studies of reaction mechanism typically concern themselves with minima and transition states on the potential energy surface (PES) for atomic nuclear motion. Free energies, when computed, are usually obtained as corrections to PES energies. In classical dynamics, however, one can envisage a free-energy surface (FES), analogous to the PES, but with minima and transition states in shifted locations. Practitioners of rate theories such as variational transition-state theory have been concerned about such shifts in transition-state locations for several years in cases where a reaction might have a "kinetic bottleneck" of importance.[1–5] When such structural shifts from PES to FES are qualitatively significant, then refined descriptions of reaction mechanism may be in order.[6,7]

We have found a case where FES minima are qualitatively shifted from the PES minima: secondary *n*-alkyl carbocations under the PW91 density-functional-theory (DFT) approximation. The main purpose of this paper is to demonstrate and analyze this shift using complementary methods. The secondary purpose of this paper is to put this result into context with other results to discuss the true structure and dynamics of *sec-n*-alkyl ions.

Secondary *n*-alkyl ions are important as short-lived intermediates in hydrocarbon reactions, such as branching rearrangement and oligomerization. Their structural anomalies are at the heart of the uncertainties[8] concerning the importance of protonated cyclopropane (PCP$^+$) intermediates in reaction mechanism. PCP$^+$ structures have some CCC bond angles of $<90°$ and are commonly seen as the lowest-energy PES minima in computational studies.[9–20] Fǎrcaşiu and co-workers[12–15] referred to them as "bridged" structures, but we prefer calling them "closed" structures, first to avoid confusion with H-bridged structures and second to recognize their dynamical relationship with classical "open" structures. We appear to be the first to point out that closed structures are rather rare in DFT simulations at catalytic (~ 800 K) temperatures.[21] This shift from closed PES to open FES structures is the focus of our study, and we limit ourselves to *sec-n*-alkyl structures.

This paper is arranged as follows. First, we catalog our results from PW91 PES geometry optimization of minimum-energy structures of *sec-n*-alkyl ions with some qualitative generalizations. Zero-point vibrational energies and free energies here are computed as traditional "static" ones using the rigid-rotor/harmonic oscillator quantum partition function computed at locations of PES minima. Second, we present results of a 150 ps PW91-based Andersen-thermostat *NVT* molecular-dynamics (MD) simulation, which demonstrates the shift from closed to open structures with elevated temperatures. Free energies here are computed using classical statistical mechanics based on observed probabilities. The two distinctly different means of computing free energies, while approximate, were both useful in studying this prevalence of open structures over closed ones in elevated-temperature simulations. Finally, we close with a catalog of our results from MP2 PES minimum-energy structures of

a)Electronic mail: allan.east@uregina.ca.
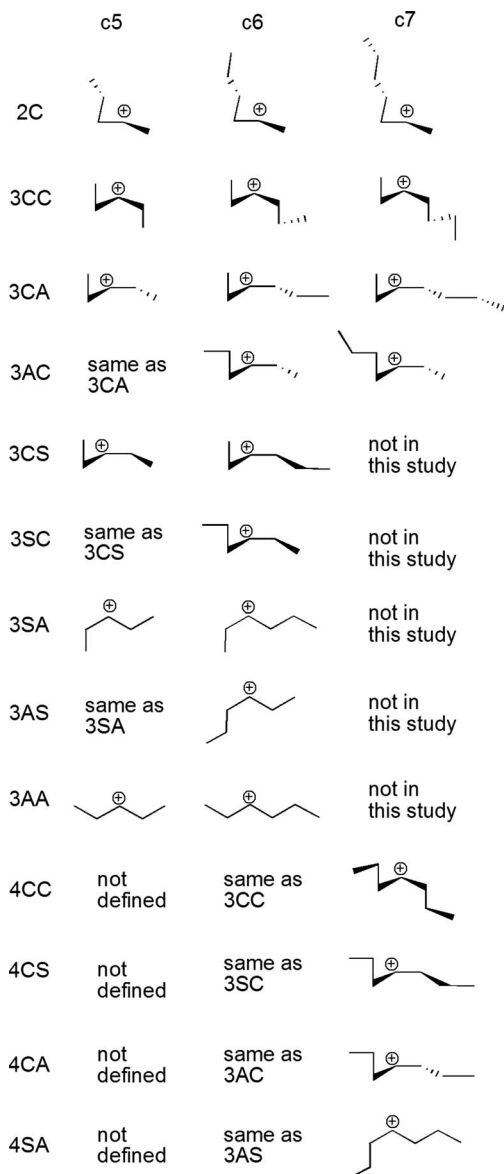
FIG. 1. Optimized conformer catalog, PW91/6-31G(d,p). *nXY* notation in the first column: *n* is the number of the charged carbon, while *X* and *Y* refer to the S/A/C positions of the subalkyl arms (see Fig. 2). *X* refers to the shorter arm for 3-hexyl and 3-heptyl ions.

sec-n-alkyl ions and discussion of how true *sec-n*-alkyl ions might behave.

II. THEORETICAL METHODS

A. Geometry optimizations

Minimum-energy structures for pentyl, hexyl, and heptyl cations were optimized with the GAUSSIAN03 computational package using its 6-31G(d,p) basis set[22] and two different levels of theory: PW91, a DFT approximation,[23] and MP2, the frozen-core Moller–Plesset perturbation theory approximation.[24] Analytic first and second derivative formulae were used for both levels of theory (save for the numerical integration grid in DFT). PES energies are reported without zero-point corrections. FES energies are computed using rigid-rotor/harmonic oscillator assumptions; note that the harmonic oscillator assumption in particular can be rather
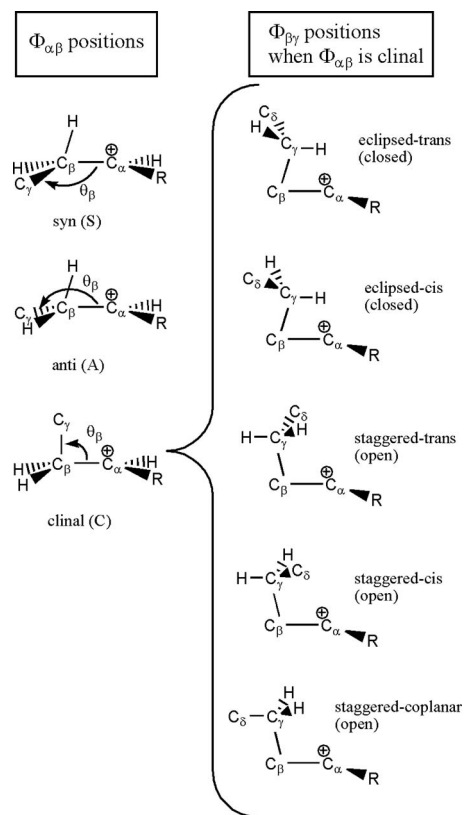
FIG. 2. Preferred dihedral-angle positions for subalkyl arms of unbranched *sec-n*-alkyl ions. First column: Possible positions for $\Phi_{\alpha\beta}(C_{\beta'}C_{\alpha}C_{\beta}C_{\gamma})$; synperiplanar, 0–10°; antiperiplanar, 130–160°; clinal, 94–104°. When $\Phi_{\alpha\beta}$ is clinal, the beta angle $\theta_{\beta}(C_{\alpha}C_{\beta}C_{\gamma})$ is considerably contracted. Second column: Possible positions for $\Phi_{\beta\gamma}(C_{\alpha}C_{\beta}C_{\gamma}C_{\delta})$ when a subalkyl arm is clinal.

poor for the entropy component of floppy vibrational degrees of freedom, such as internal rotations or low-barrier isomerization coordinates.

B. AIMD simulation

Born–Oppenheimer *ab initio* MD (AIMD) simulation was performed in the canonical *NVT* ensemble with the VASP suite[25] using the PW91 DFT approximation.[23] The projector-augmented wave (PAW) approach,[26,27] applied to pseudopotentials appropriate for generalized gradient approximation DFT,[28,29] was used for describing the interaction between core and valence electrons, and the plane-wave cutoff for valence electrons was set to 400 eV. Basis set completeness was tested by increasing the cutoff energy to 500 eV. The simulation temperature of 800 K was controlled using the Andersen thermostat[30] with a collision rate of 0.04 fs⁻¹. The atomic masses of 12.011 and 1.000 amu for C and H atoms, respectively, were used. Classical equations of motion were integrated using the Leap Frog algorithm[31] with a time step of 1 fs. The total simulation time was 150 ps. A wide cubic unit cell (13.0 Å width) was used to minimize periodic boundary effects. The charge of the cation was counterbalanced by a uniform background charge. The probability density plots were constructed using the kernel density estimation.[32] In this method, which is a generalization of a standard histogram with rectangular bins, each data point is associated with a kernel function, and the histogram is cre-

TABLE I. Optimized PW91/6-31G(d,p) structural data (angles in degrees) for sec-*n*-alkyl ions.

Conformer[a]	θ_{123}	θ_{234}	θ_{345}	θ_{456}	θ_{567}	Φ_{1234}	Φ_{2345}	Φ_{3456}	Φ_{4567}	ν_{low}[b]	E (kJ/mol)[c]
2-pentyl											
2C c5[d]	125	83	111			98	122			72	0.0
3-pentyl											
3CC c5[e]	98	126	98			101	101			79	5.7
3CS c5[f]	96	127	121			96	−1			100	6.0
3CA c5[f]	97	126	119			98	−148			62	6.6
3SA c5	121	127	120			−4	−158			106	6.3
3AA c5	119	126	119			−150	−150			76	7.4
2-hexyl											
2C c6[d]	125	84	110	111		94	132	176		41	0.0
3-hexyl											
3AC c6[d]	117	126	83	111		−144	98	122		69	−1.8
3CC c6[g]	104	125	85	111		101	99	122		53	0.2
3SC c6[d]	119	127	86	111		−8	99	120		58	0.5
3CA c6[f]	97	126	117	112		95	−137	−169		43	8.4
3CS c6[f]	96	127	121	112		97	−2	175		61	9.9
3SA c6	121	127	118	112		−5	−148	−166		28	8.3
3AS c6	120	127	122	112		−158	−5	176		65	10.0
3AA c6	114	126	126	114		−134	−172	−134		66	14.2
2-heptyl											
2C c7[d]	125	86	109	111	111	92	139	174	−178	27	0.0
3-heptyl											
3AC c7[d]	117	126	84	111	111	−144	96	127	177	48	−5.6
3CC c7[g]	104	126	86	110	111	104	95	135	176	28	−3.7
3CA c7[h]	85	126	117	112	112	94	−139	−170	−178	55	9.9
4-heptyl											
4CC c7[i]	108	101	126	101	108	177	100	100	177	49	−5.8
4CA c7[d]	111	84	126	117	112	121	98	−142	−171	59	−2.8
4CS c7[d]	111	86	127	120	112	117	99	−9	176	63	0.9
4SA c7	112	122	127	118	112	176	−6	−147	−167	33	7.9

[a]*nXY* notation (see Fig. 1).
[b]ν_{low} is the lowest vibrational harmonic frequency (cm^{-1}).
[c]E is the conformer energy relative to the corresponding 2-alkyl ion.
[d]Clinal arm is eclipsed-trans.
[e]Clinal arms are both staggered.
[f]Clinal arm is staggered.
[g]Clinal arms are staggered and eclipsed-trans.
[h]Clinal arm is eclipsed.
[i]Clinal arms are both staggered-coplanar.

ated as the normalized sum of kernel functions. To construct a two-dimensional histogram $P(x,y)$, a normal (Gaussian) kernel $K(x,y)=he^{-(x^2+y^2)/2\sigma^2}$ with $\sigma=5.7$ deg was used. Note that the value of parameter h is irrelevant as the kernel histograms are renormalized after construction.

C. Basis set equivalence

Testing was done to demonstrate that the results obtained with the PAW/plane-wave approach used in VASP are equivalent to those from the 6-31G(d,p) all-electron atom-centered basis set used in the optimizations. See Appendix for details.

III. RESULTS AND DISCUSSION

A. Optimized PW91/6-31G(d,p) structures

The PESs for *sec-n*-alkyl ions are intriguingly complex. There are a large number of minima and the conformers are not consistent from ion to ion. Figure 1 displays our structure catalog to date.

Our shorthand notation for each conformer is based on syn/anti/clinal (S/A/C) descriptions of the positions of the two "subalkyl" arms relative to the charged alpha carbon, as shown in Fig. 2. To describe proximity to the charged carbon, ensuing carbon atoms in the two subalkyl arms are labeled $\beta, \gamma, \delta, \dots$ and $\beta', \gamma', \delta', \dots$, respectively. For publica-
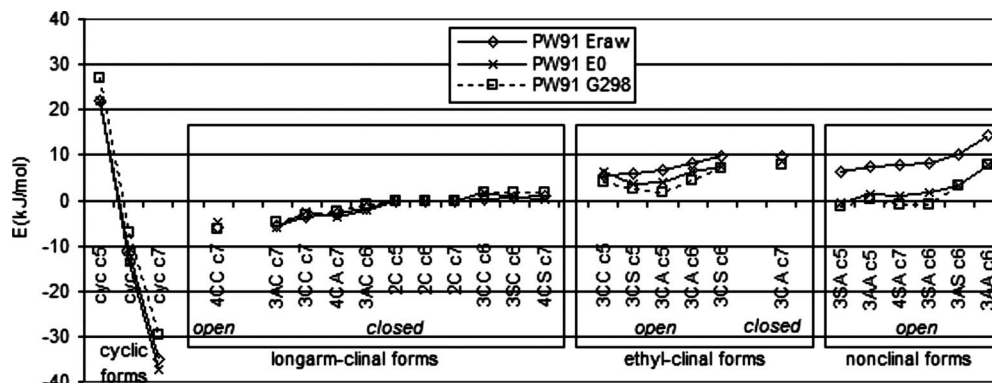
FIG. 3. Plot of PW91/6-31G(d,p) conformer energies relative to standard clinal versions of 2-pentyl, 2-hexyl, and 2-heptyl ions. E_{raw}=ground-state electronic energy, E_0=zero-point-corrected energy, and G_{298}=Gibbs free energy at 298 K in the harmonic oscillator/rigid-rotor approximations.

tion we present only one $\Phi_{\beta\gamma}$ possibility per clinal arm (generally the lowest-energy one). All other dihedral angles ($\Phi_{\beta\gamma}$ for syn and anti positions of $\Phi_{\alpha\beta}$, and other dihedral angles such as $\Phi_{\gamma\delta}$) were chosen to be near 180°.

Table I displays the quantitative results from the geometry optimizations. The angle labels in the table heading assume the carbons are numbered from end to end. The alpha angle $\theta_\alpha(C_{\beta'}C_\alpha C_\beta)$ assumes uninteresting values near 125°, but the beta angles θ_β and $\theta_{\beta'}$ show significant variation and are directly correlated with the torsion angles $\Phi_{\alpha\beta}$ and $\Phi_{\alpha\beta'}$. For synperiplanar ($\Phi_{\alpha\beta}\approx 0-10°$) and antiperiplanar ($\Phi_{\alpha\beta}\approx 130-160°$) positions, the beta angle takes expanded tetrahedral values of 117–119°, but for clinal ($\Phi_{\alpha\beta}\approx 94-104°$) positions, the beta angle *constricts greatly*, falling between 83 and 104° (Fig. 2, first column). This angle constriction for clinal positions is due to the attraction between the electron density in the "subalkyl arm" and the electrophilicity (charge and incomplete valence) of the alpha carbon and results in improved hyperconjugation of the $C_\beta C_\gamma$ bond with the empty p orbital on C_α.

Structures with clinal arms have a further complexity because they display a variety of $\Phi_{\beta\gamma}$ positions (Fig. 2, second column). At the PW91/6-31G(d,p) level of theory, the lowest-energy position for a clinal arm is normally eclipsed-trans ($\Phi_{\beta\gamma}\approx +120°$), but clinal ethyl arms seem to prefer staggered positions in 3-pentyl and 3-hexyl (although not 3-heptyl) and conformers that have two clinal arms seem to prefer having at least one staggered, with the double-clinal conformer of 4-heptyl (4CC c7) preferring both arms to be staggered-coplanar ($\Phi_{\beta\gamma}\approx 180°$). The eclipsed clinal position is able to constrict the beta angle to 83–87°, and we refer to these structures as *closed* structures. The staggered clinal position constricts the beta angle a lesser amount: to 96–98° in single-clinal structures and 101–104° in double-clinal structures, and we refer to these structures as *open-clinal*. Beta angles of 109° and beyond, found for syn and anti arms, are referred to as *open* structures.

Relative energies from the static PW91 calculations are plotted in Fig. 3. If we ignore the cyclic structures (see end of this section), then the lowest-energy forms on the PES (E_{raw}, diamonds) are ones with a clinal arm having three or more carbons ("longarm-clinal") due to maximum hyperconjugative benefit. Of these 11 structures, the lowest is the one with two clinal "longarms." Forms whose only clinal arm is ethyl ("ethyl-clinal") are higher in energy by ~10 kJ mol⁻¹ as are the classical nonclinal forms with only syn or anti arms. Note also that ten of the 11 low-energy longarm-clinal forms are also *closed forms*, thus demonstrating a general prevalence for closed forms on the PES in agreement with past studies.[9–20] Curiously, the lowest-energy form, with two clinal longarms, is *not* fully closed but open-clinal on both sides.

On the FES (Fig. 3, G298, squares), the closed longarm-clinal forms face some competition from two types of open forms. (i) Open nonclinal forms appear to have free energies commensurate with closed longarm-clinal ones, for pentyl and hexyl ions, although perhaps not for heptyl ions. The energy lowering is not only due largely to lower zero-point energies (included in E_0 in the graph) but also to greater entropy (included in G298 in the graph): the crudely com-
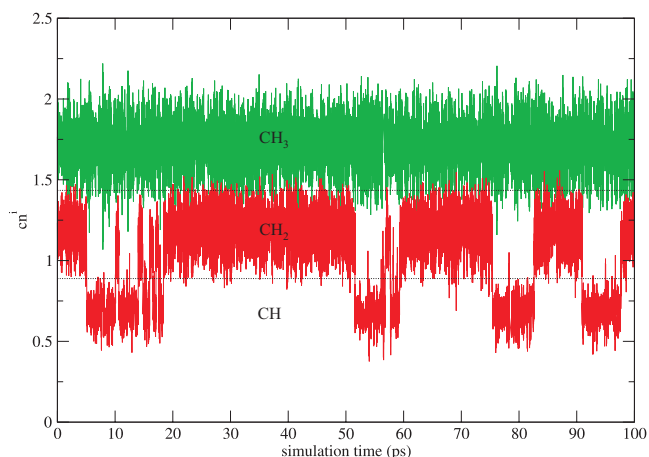
FIG. 5. Analytical function cn^i as a measure of the number of hydrogen atoms connected with carbon atom during the MD simulation. In this example, methyl group (upper curve, i=C1) was stable during whole simulation, whereas the methylene group (lower curve, carbon C5) repeatedly transformed into methine group due to spontaneous hydride transfer.

FIG. 4. Cyclic 1,5-μ-H-bridged conformers of alkyl ions from PW91 and MP2 calculations.
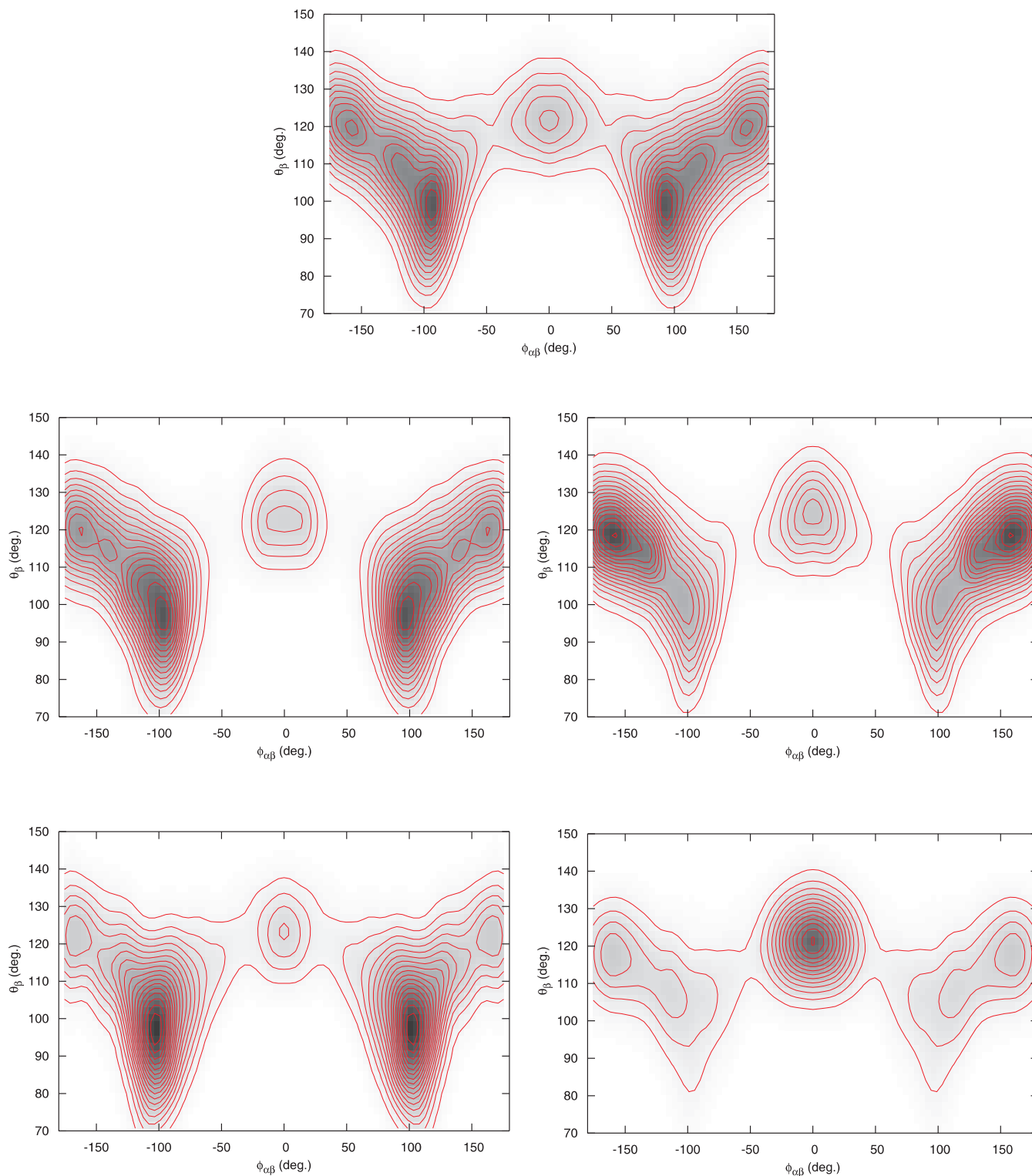
FIG. 6. Probability distributions of subalkyl arm positions of *n*-nonyl cations as a function of torsion $\Phi_{\alpha\beta}$ and angle θ_β. Statistics was increased by folding all data into the right-hand side of the plot ($0 < \Phi_{\alpha\beta} < 180°$) and making a mirror-image copy for the left-hand side ($-180° < \Phi_{\alpha\beta} < 0$). Probability increases from light to dark. Counterclockwise from bottom right: Ethyl arms of 3-nonyl, propyl arms of 4-nonyl, butyl arms of 5-nonyl, pentyl arms of 4-nonyl, and hexyl arms of 3-nonyl. Note the shift from fully open syn/anti positions to open-clinal positions as the arms become longer, with very few closed ($\theta_\beta < 90°$) structures observed.

puted entropy correction for these classical open structures provides a small further lowering for most of them at 298 K and presumably furthermore at catalytic ($\sim$800 K) temperatures. (ii) Open longarm-clinal forms also have lower free energy than their closed counterparts, although Fig. 3 can show this effect only for the "4CC c7" version.

As a side issue, Fig. 3 also plots the energies of three cyclic 1,5-μ-H-bridged isomers (Fig. 4), which we optimized but did not list in Table I. Figure 3 reveals that according to PW91, the *cyclic* structure is the most stable conformer for straight-chain alkyl ions larger than pentyl. These optimizations were motivated by the appearance of such a

TABLE II. Distribution of syn, anti-, and clinal configurations of simulated $C_9H_{19}^+$ for different charge positions and alkyl arm lengths.

Charge position/alkyl arm	Syn (%) $\|\Phi_{\alpha\beta}\| \leq 50°$	Clinal (%) $50° < \|\Phi_{\alpha\beta}\| < 130°$	Anti (%) $130° \leq \Phi_{\alpha\beta}$
C3/ethyl	41	36	23
C4/propyl	10	40	50
C5/butyl	8	49	43
C4/pentyl	7	60	33
C3/hexyl	7	73	20

structure lasting the final 40 ps of our 150 ps simulation (*vide supra*). Experimentally, μ-H-bridged structures have been observed as transannular bridges in secondary or tertiary cyocloalkyl ions,[33–36] but the secondary ion versions are difficult to detect; for instance, the $1,5$-μ-H-bridged cyclooctyl ion had a half-life of 17 min at $-142\ °C$ in $SO_2ClF-SO_2F_2$ solvent.[33]

B. *NVT* ensemble simulation of $C_9H_{19}^+$

The MD simulation started with the 5-nonyl cation. At the simulation temperature of 800 K, a large number of 1,2-H-atom shifts were observed. Thus during the initial 110 ps of simulation time the location of the three-coordinate carbon atom changed frequently. After $\sim$110 ps, a stable cyclic μ-H-bridged structure was created and remained stable during the remaining 40 ps of simulation time. As we have demonstrated in the previous section, this structure is surprisingly stable with respect to isomerization. In the following text we analyze only the first 110 ps of the MD simulation, where only acyclic conformers were present.

The location of the three-coordinated carbon atom was monitored using the function[37]

$$cn^i = \sum_{j=1}^{n_H} \frac{1 - \left(\frac{r_{ij}}{R}\right)^8}{1 - \left(\frac{r_{ij}}{R}\right)^{14}},$$

where r_{ij} is interatomic separation between carbon i and hydrogen j, R is a reference C–H bond length set to 1.1 Å, and
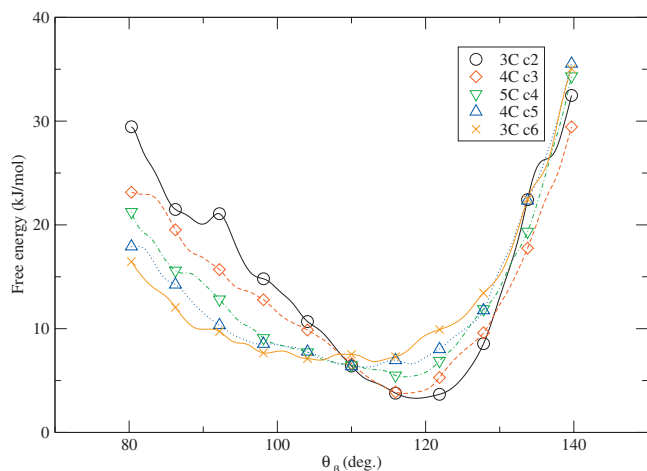
n_H is the number of hydrogen atoms in the cation. As shown in Fig. 5, the value of the function cn oscillates around 0.7 for methine, 1.2 for methylene, and 1.7 for methyl group. Terminal methyl groups were stable during the MD simulation, and hence the position of positive charge can be identified by the position of the CH group in the nonyl cation. The probability to find the CH$^+$ group at the C3, C4, or C5 positions was about the same ($\sim$30% each), but in the C2 position CH$^+$ was rarer (probability 10%).

In Fig. 6, the observed probability densities for various configurations are shown, as functions of θ_β and $\Phi_{\alpha\beta}$, for different positions of charge in the nonyl cation. These plots were made to demonstrate the predicted strong correlation of θ_β with $\Phi_{\alpha\beta}$, with θ_β constricting to 80–110° when its alkyl arm is clinal (i.e., when $\Phi_{\alpha\beta} \approx \pm 90°$). However, the data show *relatively few closed structures* (θ_β is rarely <90°), proving our claim that the FES favors open structures.

These plots provide more specific detail about this apparent shift away from closed structures. They show that as the subalkyl arms get longer (starting from the bottom right figure and moving counterclockwise), there is a gradual shift in the dihedral-angle distributions from (open) nonclinal structures to (open-) clinal ones. This shift is quantified with statistical distributions in Table II.

Hence, small subalkyl arms are generally in open positions because they are usually not clinal. Long subalkyl arms are not closed for a different reason; they are usually clinal but prefer to be open-clinal rather than closed-clinal.

FIG. 7. Helmholtz free energy of simulated $C_9H_{19}^+$ as a function of the bonding angle θ_β (see Fig. 1), calculated for various positions of charge (first number in legend) and lengths of alkyl arms (second number).
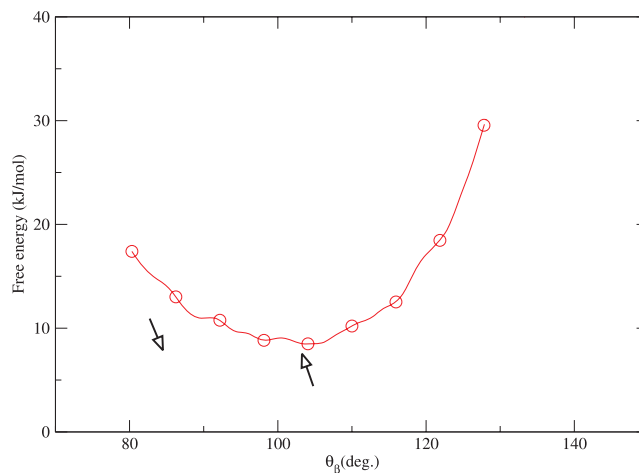
FIG. 8. Helmholtz free energy as a function of the angle $\theta_\beta = \theta_{345}$, for 3-nonyl cations whose hexyl arms are clinal. Arrow at 85° denotes expected PES minimum based on 3-heptyl results (Table I); free energy has opened this angle to $\sim$103°.

TABLE III. MP2/6-31G(d,p) structural data (angles in degrees) for sec-*n*-alkyl ions. For explanations of table headings and conformer notation, see Table I. For clinal structures (with C in the notation), the longer clinal arm is eclipsed-trans, and if a second clinal arm is present (CC structures), it is staggered-coplanar.

Conformer	θ_{123}	θ_{234}	θ_{345}	θ_{456}	θ_{567}	Φ_{1234}	Φ_{2345}	Φ_{3456}	Φ_{4567}	ν_{low}	E (kJ/mol)
2-pentyl											
2C c5	124	78	109			98	122			101	0.0
3-pentyl											
3CA c5	77	125	115			97	−144			111	6.8
3CC c5	106	124	79			100	97			101	7.5
3CS c5	79	126	118			98	−13			104	10.2
3AA c5	125	125	113			−173	−131			102	14.5
3SA c5	117	126	124			−8	−172			131	15.0
2-hexyl											
2C c6	124	78	109	111		97	125	178		82	0.0
3-hexyl											
3AC c6	115	125	78	110		−145	98	121		98	−1.1
3CC c6	106	124	79	109		98	99	122		73	−0.1
3SC c6	117	126	79	110		−14	100	118		89	2.5
3CA c6	78	125	116	112		96	125	−172		86	10.1
3CS c6	79	126	118	111		98	−13	177		78	14.2
3AA c6	113	125	125	113		−132	−174	−132		67	15.3
3SA c6	116	126	125	113		−10	−173	−132		84	15.6
3AS c6	124	126	117	111		−172	−9	−180		98	19.1
2-heptyl											
2C c7	124	77	109	111	112	97	125	178	−178	57	0.0
3-heptyl											
3AC c7	115	125	77	110	111	−144	98	123	179	73	−5.3
3CC c7	106	124	78	109	111	99	98	125	178	59	−4.2
3CA c7	78	125	115	112	112	96	−141	−171	−179	69	11.0
4-heptyl											
4CC c7	110	80	125	106	110	123	99	98	179	59	−2.5
4CA c7	110	78	125	115	112	121	98	−143	−173	73	−2.0
4CS c7	110	79	126	118	111	118	100	−14	177	76	2.2
4SA c7	111	117	126	125	113	−179	−10	−173	−132	78	15.4

One can plot Helmholtz free energy versus θ_β via $A(\theta_\beta)=-k_BT \ln p(\theta_\beta)$, where $p(\theta_\beta)$ is the probability to find angle θ_β at a certain specific value. Such free-energy profiles calculated for various positions of charge in nonyl cation and lengths of alkyl arms next to the CH$^+$ group are shown in Fig. 7. We find that the free-energy minimum corresponds to an open structure ($\theta_{\beta,\min}>90°$) for each configuration. For small subalkyl arms the minimum is 117–119°, suggestive of nonclinal structures. For longer arms, the width of the free-energy valley gets wider and the minimum shifts to 105–115°, suggestive of a structural shift toward open-clinal structures.

Finally we should eliminate the possibility that the open-clinal structures that dominate the simulation might be due solely to structures that are open-clinal on both the PES and FES, such as the double longarm-clinal structure 4CC c7 in Fig. 3. Figure 8 plots the free energy only for 3-nonyl ions having clinal hexyl arms, as functions of $\theta_\beta=\theta_{345}$. 3-Nonyl

ions have a clinal hexyl arm 73% of the time (Table II). Figure 8 clearly shows that these clinal ions prefer $\theta_\beta>90°$ on the FES, whereas the PESs for the closest analogs in Table I (3AC c7 and 3CC c7) give $\theta_\beta=84–86°$.

C. Other effects on open versus closed structures

Here we will discuss whether this dynamic shift from closed to open structures on the high-temperature FES will be altered if we consider the effects of improving the level of theory for electronic energy and possible solvation effects. Since AIMD simulations cannot currently be performed with alternative levels of theory, we chose to compare the effects of PES structures with level of theory. We reoptimized all structures in the catalog with MP2 rather than PW91 DFT, and the results appear in Table III.

Of the qualitative differences between PW91 and MP2,

the largest one is in the nonclinal structures: PW91 predicts classical three-coordinate alpha carbons, while MP2 predicts *nonclassical* H-*bridged structures* (employing a H atom from a C_β or $C_{\beta'}$ clinal position). Changes in the preferred beta angles are minor: (i) for synperiplanar ($\Phi_{\alpha\beta} \approx 0°$) and anti-periplanar ($\Phi_{\alpha\beta} \approx \pm 150°$) positions, the beta angles of 117–122° (PW91) become 115–118° (MP2); (ii) for eclipsed clinal positions, the beta angles of 83–87° (PW91) become 77–80° (MP2); (iii) for staggered clinal positions in double-clinal forms, the beta angles of 101–104° (PW91) become 106–107° (MP2). For clinal arms, PW91 gave a milder preference for (closed) eclipsed positions versus (open) staggered ones, unless the clinal arm was an ethyl arm; MP2 gives a stronger preference to closed eclipsed positions, even for ethyl arms, and tightens the beta angle of such positions, almost achieving true μ-alkyl bridging.

The relative energies of the MP2 structures are plotted in Fig. 9 for the same conformers as presented in Fig. 3 (and in the same order). MP2 disagrees with PW91 on the energies of the nonclinal open forms as well as the structures, placing their raw energies 5–8 kJ higher than those of the ethyl-closed forms and placing their zero-point-corrected and free energies near those of the ethyl-closed forms. Hence, according to MP2, open forms (whether clinal or nonclinal) *might not* have lower free energy than the longarm-closed forms in the plot, and hence MP2-based simulations (were they possible today) might reveal substantially more closed structures.

Which is more likely to be correct, the PW91 picture with few closed structures, or the MP2 picture with substantially more? PW91 is a "semilocal" DFT, which therefore lacks long-range electron correlation and hence will poorly estimate long-range interactions,[38] such as dispersion or other effects that may be important in stabilizing the closed structures. However, MP2 with small basis sets is known to excessively stabilize bridged structures[10] due to overcorrection of the correlation effect[39] and perhaps enhanced basis set superposition error.[40] At higher accuracy, Fărcaşiu pointed out that CCSD optimizations of a branched *sec*-alkyl ion indicate that the preference for closed forms lies intermediate between the DFT and MP2 results.[15] Hence, this PES effect, which further lowers closed-structure energies, might cause

the open and closed forms of *sec-n*-alkyl ions to have commensurate free energies in reality.

Another issue is possible solvation effects. Fărcaşiu was concerned for many years about the role of ion-pairs in the formation of alkyl ions in superacidic molecular liquids and suggested that the nearby presence of an anion "partner" could be causing open-form secondary ions as intermediates. For instance, he performed restricted optimizations of the structures of several small alkyl ions in ion-pair complexes with the approaching and weakly nucleophilic H_3BF^- ion[13,14,41,42] and found that open structures become lower in energy than closed ones on the PES once the anion approaches within ~3 Å of the cation. In contrast, one of us has done unrestricted optimizations of complexes of closed-structure alkyl ions with NH_3,[17] H_2O,[17] HF,[17] $AlHCl_3^-$,[18] $AlCl_4^-$,[18,19] $Al_2Cl_7^-$,[20] and various small zeolite fragment ions,[19,20] and no structure-opening was seen unless the alkyl ion became covalently bonded to the nucleophile. We see open secondary ions, without ion-pairing, in our simulations of alkyl ions in zeolites or ionic liquids at catalytic temperatures. Hence, the prevalence of open structures in simulations with catalysts could be a solvation effect, but it could also be a free-energy effect as seen in our gas-phase simulation, and both possibilities should be considered.

Hence, the preference for closed structures on the PW91 PES is reversed by dynamical effects (zero-point and free-energy corrections), and although PW91 neglects weak intramolecular interactions, these weak interactions might be counterbalanced to some extent by intermolecular interactions with solvent/catalyst, which are also absent in the calculations here. The grander issue of whether the open structures seen in simulations are real or not appears to be (pun not intended) an open one.

D. The cyclic structure

Both MP2 and PW91 optimizations give evidence that the cyclic conformers are lower in free energy than both open and closed structures for *sec-n*-alkyl ions larger than hexyl ion. However, in polar solutions or ionic liquids, there is a noticeable solvation effect that may make the cyclic and acyclic forms commensurate in energy. A computational study of cyclic tertiary (not secondary) alkyl ions by Vrček *et*
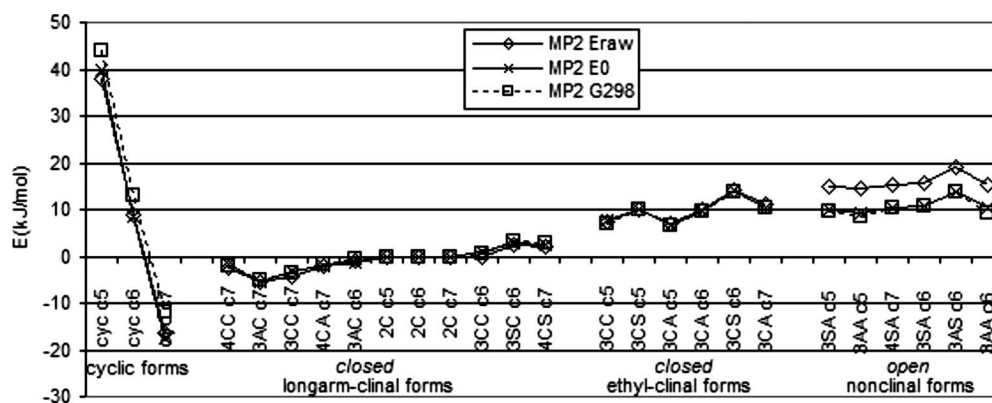
FIG. 9. Plot of MP2/6-31G(d,p) conformer energies relative to standard clinal versions of 2-pentyl, 2-hexyl, and 2-heptyl ions. E_{raw}=ground-state electronic energy, E_0=zero-point-corrected energy, and G_{298}=Gibbs free energy at 298 K in the harmonic oscillator/rigid-rotor approximations.

TABLE IV. Optimized beta angles and dihedrals (degrees), 5-nonyl ion, GAUSSIAN03 vs VASP.

Conformer[a]	Basis set[b]	θ_{345}	θ_{567}	Φ_{3456}	Φ_{4567}
5AC	6-31G(d,p)	117	89	−138	94
5AC	Prec=normal, 400 eV	117	86	−143	95
5AC	Prec=high, 500 eV	117	85	−141	95
5CC	6-31G(d,p)	100	100	100	100
5CC	Prec=normal, 400 eV	100	101	100	100
5CC	Prec=high, 500 eV	100	100	100	100
5SC	6-31G(d,p)	121	97	−1	−95
5SC	Prec=normal, 400 eV	121	97	−2	−95
5SC	Prec=high, 500 eV	121	96	−1	−95
Snapshot9	Starting structure	118	113	24	132
Snapshot9	Prec=low, 300 eV	125	115	20	137
Snapshot9	Prec=normal, 400 eV	120.5	98.1	11.0	93.3
Snapshot9	Prec=high, 500 eV	120.5	97.9	11.1	92.6
Snapshot9	6-31G(d,p)	120.4	98.2	11.2	91.7
Snapshot9	6-31G(d,p) ultrafine[c]	120.4	98.1	11.8	91.7
Snapshot9	cc-pVTZ	120.6	98.3	9.9	93.0

[a]Subalkyl arms are all-trans except for snapshot9.
[b]6-31G(d,p) and cc-pVTZ are all-electron atom-centered basis sets used with GAUSSIAN03, which provide 230 and 536 basis functions (respectively) for $C_9H_{19}{}^+$; prec=x,y indicate pseudopotentials with plane-wave basis sets, used with VASP, in which y specifies the upper limit (ENCUT) for plane waves supplied.
[c]Ultrafine: A finer numerical integration mesh (grid=ultrafine).

al.[43] using polarizable continuum methods ($\varepsilon=30$) found a relative stabilization effect of $6-11$ kcal mol^{-1} that moved the open tertiary cation structure lower in energy than the cyclic one. We have performed simulations of 2,6-H-bridged nonyl ion in the ionic liquid $[C_5H_5NH^+][Al_2Cl_7{}^-]$ and observed interconversions (within 4 ps time windows) of cyclic and acyclic structures between 500 and 1200 K, also suggesting a destabilization of the cyclic structure vis-à-vis our 800 K gas-phase simulation reported in Sec. III B. While this curious structure should be worthy of further study, it may not be important for chemical mechanism since no tendency to fully connect the 1,5 C–C bond was observed in the simulations.

IV. CONCLUSIONS

With the PW91 approximation for energy, there is a shift from closed (PCP$^+$) to open structures for a gas-phase secondary *n*-alkyl ion when going from the PES to a FES at catalytic (800 K) temperatures. The nature of this opening depends on the lengths of the subalkyl arms; longer arms prefer open-clinal positions and less energy to close, while shorter arms prefer open nonclinal positions (particularly ethyl and perhaps propyl arms) and require more energy to close. The reason for the structural opening from PES to FES is primarily entropic, except for hexyl or pentyl ions in which the lowered zero-point energy for nonclinal open structures appears to be the reason.

In reality, the preference for open structures on the FES may not be as strong as seen in PW91-based MD simulations since in static MP2 calculations, the preference for closed structures is more pronounced than in PW91 ones and more accurate energies might suggest more equal probabilities for open and closed structures. The effect of particular solvents and catalysts on the open/closed question may be important as well.

The PW91-based MD simulation also led to the discovery that $1,5$-μ-H-bridged alkyl ion structures are low in energy for *n*-alkyl ions longer than hexyl and that such structures may in fact dominate the very brief lifetimes of secondary *n*-alkyl ions in the gas phase, although perhaps not in strongly polar or ionic solvents.

APPENDIX: BASIS SET EQUIVALENCE

Geometry optimizations of four initial structures of 5-nonyl ions were performed with both GAUSSIAN03 and VASP, and the results are tabulated (see Table IV). The 400 eV plane-wave set and the 6-31G(d,p) atom-centered set were seen to be sufficient to reproduce large-basis results for geometrical parameters of secondary *n*-alkyl ions.

[1]B. C. Garrett and D. G. Truhlar, J. Am. Chem. Soc. **102**, 2559 (1980).
[2]S. K. Gray, S. A. Rice, and M. J. Davis, J. Phys. Chem. **90**, 3470 (1986).
[3]D. Chandler and R. A. Kuharski, Faraday Discuss. Chem. Soc. **85**, 329 (1988).
[4]S. J. Klippenstein and R. A. Marcus, J. Phys. Chem. **92**, 3105 (1988).
[5]S. J. Klippenstein, A. L. L. East, and W. D. Allen, J. Chem. Phys. **101**, 9198 (1994).
[6]S. C. Ammal, H. Yamataka, M. Aida, and M. Dupuis, Science **299**, 1555 (2003).
[7]S.-Y. Yang, P. Fleuriat-Lessard, I. Hristov, and T. Ziegler, J. Phys. Chem. A **108**, 9461 (2004).

[8] M. B. Smith and J. March, *March's Advanced Organic Chemistry*, 5th ed. (Wiley, New York, 2001).

[9] P. C. Hariharan, L. Radom, J. A. Pople, and P. R. Schleyer, J. Am. Chem. Soc. **96**, 599 (1974).

[10] S. Sieber, P. Buzek, P. R. Schleyer, W. Koch, and J. W. de M. Carneiro, J. Am. Chem. Soc. **115**, 259 (1993).

[11] M. Boronat, P. Viruela, and A. Corma, J. Phys. Chem. **100**, 16514 (1996).

[12] D. Fărcaşiu and S. H. Norton, J. Org. Chem. **62**, 5374 (1997).

[13] D. Fărcaşiu and D. Hâncu, J. Am. Chem. Soc. **121**, 7173 (1999).

[14] D. Fărcaşiu, S. H. Norton, and D. Hâncu, J. Am. Chem. Soc. **122**, 668 (2000).

[15] D. Fărcaşiu, P. Lukinskas, and S. V. Pamidighantam, J. Phys. Chem. A **106**, 11672 (2002).

[16] C. C. J. Fouillet and J. Mareda, J. Mol. Struct.: THEOCHEM **589–590**, 7 (2002).

[17] K. C. Hunter, C. Seitz, and A. L. L. East, J. Phys. Chem. A **107**, 159 (2003).

[18] Q. Li, K. C. Hunter, and A. L. L. East, J. Phys. Chem. A **109**, 6223 (2005).

[19] Q. Li and A. L. L. East, Can. J. Chem. **83**, 1146 (2005).

[20] Q. Li and A. L. L. East, Can. J. Chem. **84**, 1159 (2006).

[21] A. L. L. East, T. Bucko, and J. Hafner, J. Phys. Chem. A **111**, 5945 (2007).

[22] M. J. Frisch, G. W. Trucks, H. B. Schlegel *et al.*, GAUSSIAN 03, Revision C.02, Gaussian, Inc., Wallingford, CT, 2004.

[23] J. P. Perdew, J. A. Chevary, S. H. Vosko, K. A. Jackson, M. R. Pedersen, D. J. Singh, and C. Fiolhais, Phys. Rev. B **46**, 6671 (1992).

[24] C. Møller and M. S. Plesset, Phys. Rev. **46**, 618 (1934).

[25] G. Kresse and J. Furthmüller, Phys. Rev. B **54**, 11169 (1996).

[26] P. E. Blochl, Phys. Rev. B **50**, 17953 (1994).

[27] G. Kresse and D. Joubert, Phys. Rev. B **59**, 1758 (1999).

[28] D. Vanderbilt, Phys. Rev. B **41**, 7892 (1990).

[29] G. Kresse and J. Hafner, J. Phys.: Condens. Matter **6**, 8245 (1994).

[30] H. C. Andersen, J. Chem. Phys. **72**, 2384 (1980).

[31] R. W. Hockney and J. W. Eastwood, *Computer Simulations Using Particles* (McGraw-Hill, New York, 1981).

[32] B. W. Silverman, *Density Estimation for Statistics and Data Analysis* (Chapman and Hall, London, 1986).

[33] R. P. Kirchen and T. S. Sorensen, J. Am. Chem. Soc. **101**, 3240 (1979).

[34] R. P. Kirchen, K. Ranganayakulu, B. P. Singh, and T. S. Sorensen, Can. J. Chem. **59**, 2173 (1981).

[35] J. E. McMurry, T. Lectka, and C. N. Hodge, J. Am. Chem. Soc. **111**, 8867 (1989).

[36] M. Saunders and H. A. Jimenez-Vazquez, Chem. Rev. (Washington, D.C.) **91**, 375 (1991).

[37] M. Iannuzzi, A. Laio, and M. Parrinello, Phys. Rev. Lett. **90**, 238302 (2003).

[38] F. O. Kannemann and A. D. Becke, J. Chem. Theory Comput. **5**, 719 (2009).

[39] K. Raghavachari, R. A. Whiteside, J. A. Pople, and P. R. Schleyer, J. Am. Chem. Soc. **103**, 5649 (1981).

[40] A. E. Shields and T. van Mourik, J. Phys. Chem. A **111**, 13272 (2007).

[41] D. Fărcaşiu and D. Hâncu, J. Phys. Chem. A **101**, 8695 (1997).

[42] D. Fărcaşiu and R. Leu, J. Phys. Chem. A **112**, 2955 (2008).

[43] V. Vrček, I. Vinkovič Vrček, and H.-U. Siehl, J. Phys. Chem. A **110**, 1868 (2006).